Characterizing Particle Size, Water Path and Photon Tunneling in Ice and Water Clouds

David L. Mitchell
Atmospheric Sciences Division
Desert Research Institute
Reno, Nevada

Robert P. d'Entremont
Satellite Meteorology Group
Atmospheric and Environmental Research, Inc.
Lexington, Massachusetts

Abstract

Global information of ice water path (IWP) in ice clouds is urgently needed for testing of global climate models (GCMs) and other applications, but satellite retrievals of IWP are still in the developing stages, and tend to have large uncertainties (e.g. factor of 3 or more). Results of a new retrieval method are presented here that may have relatively low uncertainties, using several thermal-radiance channels.

Recent research indicates that ice-cloud radiative properties depend on more than effective diameter (D_{EFF}) and ice water content (IWC). The size distribution shape, or dispersion, such as the degree of bimodality, is also an important factor at thermal wavelengths. On the other hand, based on new information on ice particle mass- and area-dimensional relationships, ice particle shape uncertainties now appear to have minimal adverse influence on IWP retrievals.

Consequently, we have developed a retrieval scheme that accounts for the size distribution (SD) shape in mid-latitude and tropical cirrus. By using a channel centered near 3.9 μm, absorption is largely a volume-dependent radiative process. This reduces particle shape uncertainties, which are associated with area-dependent absorption. Radiation-transfer model simulations that vary particle size, IWC and cloud depth suggest our IWP retrieval scheme is accurate to about ±15% over an IWP range of 1 to 100 g m^{-2}, and about ±25% over an IWP range of 100 to 200 g m^{-2}, except for very thin cirrus having unusually large crystals or multiple cloud layers.

Retrieval results with ground-based AERI data are presented for ARM cirrus IOPs of 9 and 13 March 2000. IWP retrievals are compared with in-situ aircraft data, and coincident GOES retrievals are presented as well.

Finally, our scheme is equally well suited for water clouds for determining LWP. Uncertainties are lower since absorption in water clouds at 3.9 μm is about half that for ice clouds, and there is no uncertainty due to particle shape. We will present sensitivity simulations of LWP retrievals using AERI radiances, and show preliminary results for some water-droplet-cloud cases.

Why are SD Shape, Ice Water Path and Effective Size Important?

Satellite and ground-based retrievals of cirrus effective diameter (D_{EFF}) and ice water path (IWP) are needed to describe their radiative properties and evaluate their influence on radiative forcing and climate. Unfortunately these properties are not sufficient for describing the radiative behavior of cirrus at terrestrial wavelengths. Size distribution (SD) shape must also be known for terrestrial radiation. For example, the absorption optical depth may differ up to 44% for two cirrus size distributions having the same D_{EFF} and IWP.

Even knowing the size distribution shape is not totally sufficient for describing the radiative nature of cirrus clouds at infrared wavelengths. This is because a process called photon tunneling often contributes significantly (between 15 and 42%) to the absorption of infrared energy by cirrus ice particles, as shown in below. Tunneling here labels the process by which photons beyond the particle's geometric cross-section are absorbed, in comparison to absorption due strictly to the particle's geometric cross section or internal reflection/refraction. Contributions to tunneling are greatest when particle size and wavelength are comparable.

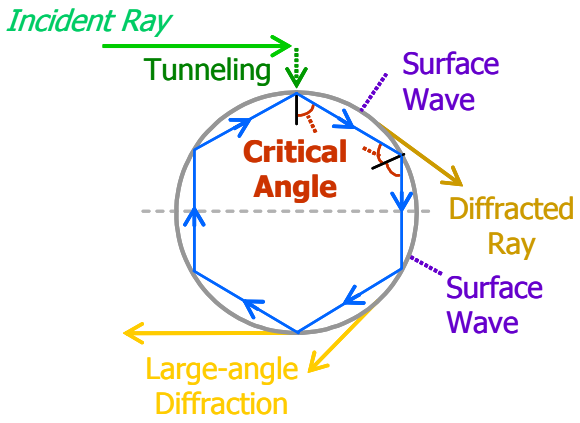

Tunneling has been parameterized for ice clouds by Mitchell (2000), whose radiation scheme was found to be accurate within 15% relative to T-matrix calculations of absorption efficiency (5% mean error) over the wavelength range 2-18 μm. Additionally, mean extinction efficiency (Q_{EXT}) errors for a hexagonal-column ice cloud were ≤3% relative to measured Q_{EXT} over the same wavelength range (Mitchell, 2001). Hence it appears justifiable to use this radiation scheme, making it necessary to retrieve the tunneling factor t_f, which ranges between 1 (for ice spheres) and 0 (no tunneling).

We present here the first estimates of tunneling in natural cirrus, which in turn provides for a physically consistent retrieval of D_{EFF} and IWP based on the second (area) and third (mass) moments of the ice-particle size distribution N(D). These retrievals are sensitive to the small-particle mode of N(D) (i.e., D

< 100 μm), which radar retrievals may not be sensitive to. We show here cirrus retrievals that are both ground- and satellite-based.

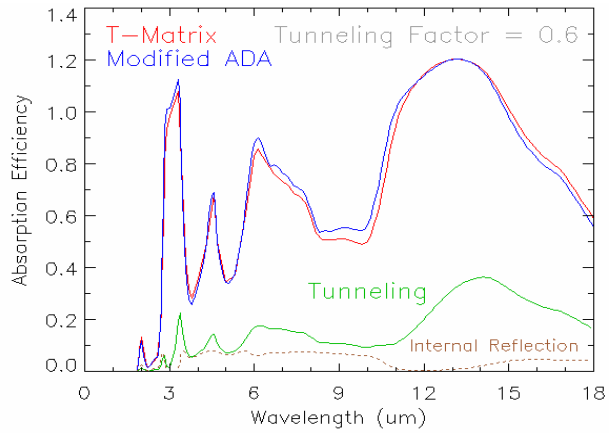

Ground-Based Retrievals

Cirrus emissivities, and hence τ_{ABS}, can be obtained spectrally from the Atmospheric Emitted Radiance Interferometer (AERI), as described in DeSlover et al. (1999). While previous studies have used the ratio $\alpha = Q_{EXT}(\text{Visible}) / Q_{ABS}(\text{TIR})$ of visible extinction efficiency to thermal absorption optical thickness to infer D_{EFF}, we find that the mismatch between the radiometer/ interferometer and lidar FOVs may lead to large errors in this ratio. By using one instrument with one FOV, this error is eliminated. Rather than using the "α" ratio, we use ratios of absorption optical thickness τ_{ABS}, for various microwindows of the upward-looking AERI instrument.

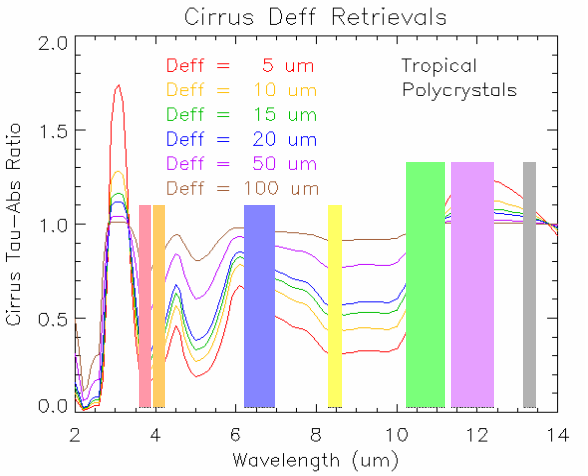

By ratioing AERI absorption optical thickness combinations of 3.9/10.1 μm, or 3.9/11.2 μm, it is possible to retrieve D_{EFF}, as shown above (plot, top of next column). These curves were generated using the ice-cloud radiation model described in Mitchell (2002), assuming N(D) for both tropical and mid-latitude cirrus, and for shapes that include rosettes, plates, hexagonal columns, and planar polycrystals. Mitchell (2002) describes that size distributions with differing D_{EFF} values can have the same radiative

properties because of the behavior of the small- and large-particle modes. These curves provide insight to expected retrieval accuracies of D_{EFF}. Size information is best obtained when using infrared bands where absorption is volume- (mass) dependent, such as at 3.9 μm. At 10.1 μm, absorption is partially mass and partially area-dependent, but is strongly area-dependent at 11.2 μm.

Ground-Based AERI and Satellite-Based Retrievals

The τ_{ABS} ratio plot also has applications to ground-based AERI and satellite retrievals. The Terra MODIS and GOES Imager instruments have channels at 3.74, 4.05, 8.55, 11, and 12 μm, similar to the bands denoted above. Cirrus emissivity is estimated using a coupled algorithm that simultaneously retrieves ice-water path, ice-crystal particle size, emissivity, and cirrus temperature using radiances collected in the mid-wave infrared (MWIR), water-vapor (WV), and thermal infrared (TIR) wavelengths, nominally at 3.9, 6.7, and 10.8 μm. Cirrus IWP, emissivity, effective particle size, and effective temperature (defined here as the temperature of the radiative "center of mass" of the cirrus cloud) are interdependent from a radiative transfer purview. The fundamental non-uniqueness of the relationship between measured radiance and cloud IWP, emissivity, particle size, and temperature at a single wavelength is resolved by forcing the retrieved parameters to be simultaneously consistent with theory and satellite observations at multiple infrared wavelengths.

Ice Crystal Cloud Emissivity and Temperature

Uncertainties in cirrus retrievals are to first order due to the fact that observed cirrus radiances are influenced by both cloud and the cloud-free atmosphere. The downwelling thermal radiance J_{OBS} measured by a ground-based sensor for a field of view completely filled by a cloud is well approximated by

$$J_{OBS} = t_{CLD}\, J_A\, \tau_B + J_B + \varepsilon_{CLD}\, B(T_{CLD})\, \tau_B + r_{CLD}\, B(T_{SFC})\, \tau_B^2 \qquad (1a)$$

where J_{OBS} is the downwelling AERI-observed radiance; t_{CLD}, ε_{CLD}, and r_{CLD} are the cloud transmissivity, emissivity, and reflectivity, respectively, and depend on the cloud effective particle size D_{EFF} and size distribution N(D); $B(T_{CLD})$ denotes the cloud blackbody radiance; J_A (J_B) denotes the downwelling radiance emitted by the non-cloudy atmosphere above (below) the cloud layer; and where τ_B is the atmospheric transmittance between cloud base and the ground.

The upwelling thermal radiance I_{OBS} measured by a satellite sensor for a field of view completely filled by a non-reflective thin cirrus cloud is well approximated by

$$I_{OBS} = t_{CLD}\, I_{SFC} + \varepsilon_{CLD}\, B(T_{CLD})\, \tau_A + r_{CLD}\, I_A\, \tau_A \ , \qquad (1b)$$

where the set {ε,r,t} of cloud radiative attributes is as for Eq. (1a); I_{SFC} is the upwelling radiance emitted by the underlying surface (i.e., either the ground or an underlying cloud deck) and clear atmosphere; $B(T_{CLD})$ denotes the cloud blackbody radiance; I_A denotes the downwelling radiance emitted by the non-cloudy atmosphere above the cloud layer; and where τ_A is the atmospheric transmittance between cloud top and TOA.

The two unknowns of interest in Equations (1a) and (1b) are the cloud radiative properties {ε,r,t} (a function of D_{EFF}) and the cloud Planck blackbody emission $B(T_{CLD})$, which is a known function of the cloud effective temperature T_{CLD}. Retrieval of these two unknowns is achieved by considering Eqs. (1a) or (1b) for simultaneous radiance measurements at two infrared wavelengths, resulting in a system of two equations in two unknowns. This process is illustrated graphically in the following two figures.

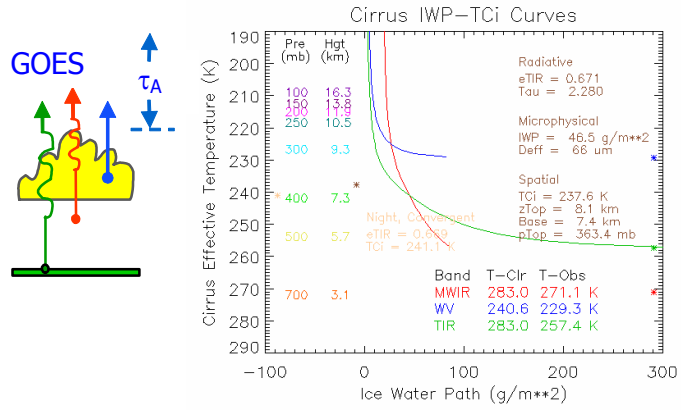

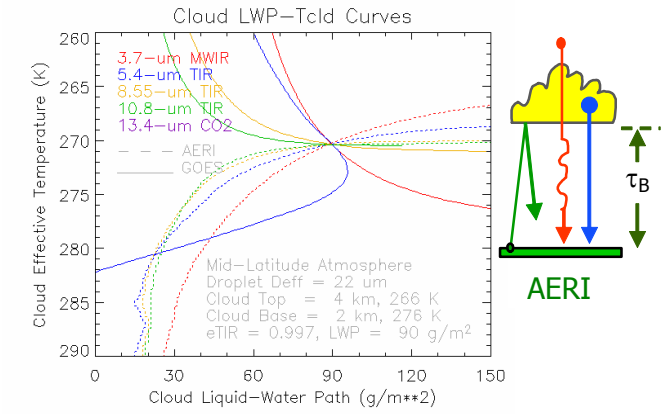

Ice Crystal Effective Diameter and IWP

By way of introduction, retrieved temperatures and TIR emissivities can be converted to visible optical thickness τ, IWP, and D_{EFF} using the theory described in this section. Cirrus ice-crystal effective diameter D_{EFF} is an important cloud attribute in our cloud retrieval approach, and is directly related to ice water content (IWC).

It can be shown that the effective diameter D_{EFF} for a size distribution of ice crystals is

$$D_{EFF} = 3\ IWC / (2\ \rho_i\ P_T) , \qquad (2)$$

where IWC is the cirrus ice water content (mass per unit volume), ρ_i is the density of ice, and P_T is the total projected area of all ice crystals in the size distribution. Projected area P_T has units of area per unit volume, or inverse length.

The coefficient for absorption is defined as

$$\beta_{ABS} = \int_0^\infty Q_{ABS}(D, \lambda)\, P(D)\, N(D)\, dD\,, \tag{3}$$

where Q_{ABS} is the absorption efficiency at wavelength λ for ice crystals of maximum dimension D, P(D) is the projected area for a crystal of maximum dimension D, and N(D) is the ice-crystal particle size distribution. N(D) has units of "per unit volume per unit length;" Q_{ABS} is dimensionless (the ratio of the radiative and geometric cross sections). It follows that the absorption coefficient β_{ABS} has units of inverse length.

We can solve for the ice water path (IWP) in terms of Q_{ABS} if we define a Q_{ABS} for the entire size distribution N(D):

$$\beta_{ABS} = \bar{Q}_{ABS}\, P_T\,, \tag{4}$$

where P_T is the geometric cross section for the entire size distribution and β_{ABS} and P_T depend on whether the cirrus are diagnosed as either convective or non-convective in origin. In this calculation, P_T is also implicit in β_{ABS}, and Q_{ABS} is independent of P_T (and the IWC assumed to calculate P_T). However, Q_{ABS} must be theoretically consistent with the retrieved values for D_{EFF}, and this is insured through our ice cloud radiation scheme for the diagnosed N(D) shape.

Equation 4 can now be combined to solve for the ice water path IWP, which is the ice mass per unit area of a vertical column through the cirrus cloud. By definition, and assuming that IWC is the vertically averaged value,

$$IWP = IWC\, \Delta z \tag{5}$$

and Eq. (2) becomes

$$D_{EFF} = 3\, IWP / (\, 2\, \rho_i\, P_T\, \Delta z\,)\,, \tag{6}$$

giving

$$IWP = 2\, \rho_i\, D_{EFF}\, \tau_{ABS} / (3\, \bar{Q}_{ABS}\,) \tag{7}$$

with the help of Eq. (4) solved for P_T, along with the definition of absorption optical depth $\tau_{ABS} = \beta_{ABS}\, \Delta z$ for a cirrus cloud where the size distribution N(D) is invariant with in-cloud position.

Assuming no scattering at infrared wavelengths the cirrus emissivity is

$$\varepsilon = 1 - \exp(\, -\tau_{ABS} / \cos\theta_{SAT}\,)\,, \tag{8}$$

where θ_{SAT} is the satellite zenith angle. Substituting for τ_{ABS} in Eq. (8) using Eq. (7) yields

$$IWP = -2\,\rho_i\,D_{EFF}\cos\theta_{SAT}\ln(1-\varepsilon)\,/\,(3\,\bar{Q}_{ABS})\,. \quad (9)$$

Fortunately, we have exploited a means for estimating N(D) in tropical anvil and mid-latitude cirrus as a function of cirrus environmental temperature, while D_{EFF} is retrieved using the τ_{ABS} ratios 3.74/11.2 and 3.74/8.55 μm. Knowing D_{EFF}, the absorption efficiency Q_{ABS} is solved for using these N(D) parameterizations and the ice-cloud radiation scheme of Mitchell (2002). It is important to note Q_{ABS} is a function of ice particle shape, wavelength, refractive index, and N(D) dispersion (i.e., the degree of bimodality).

Results

AERI Retrievals

Once D_{EFF} is retrieved, the tunneling factor t_F can be estimated from the retrieved AERI τ_{ABS} normalized to the τ_{ABS} having greatest absorption. This is shown for the 8-13 μm region in the Figure at the top of the next page. The AERI data, denoted as "x", are for the 10 Nov 95 cirrus case described in DeSlover et al. (1999), while the solid curve is the best fit to the AERI data, and was predicted by the Mitchell (2002) algorithm for $t_F = 0.3$ and $D_{EFF} = 65$ μm. The short-dashed curve predicts normalized τ_{ABS} for $t_F = 0$, while the long-dashed curve is for $t_F = 1$ (maximum value). This illustrates how radiances between 10.5 and 11.7 μm are sensitive to the value of t_F, and can be used to estimate the tunneling factor itself. AERI data at $\lambda < 10.1$ μm are much less sensitive to t_F, but is sensitive to D_{EFF}. The five data points above the predicted curves in the 8.5-9.3-μm region are unexplained based on our knowledge of ice refractive indices, and these points were persistently high in the AERI samples.

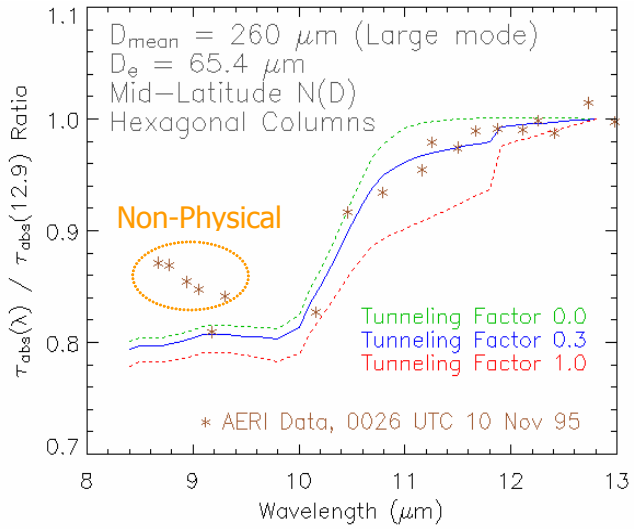

The AERI retrievals from 10 Nov could be explained using either the mid-latitude N(D)s of Ivanova et al. (2001), but only if one assumes hexagonal columns; or by the tropical N(D)s of Mitchell et al. (2000) assuming planar polycrystals. In this analysis, we chose to use the mid-latitude parameterizations

because of the location of the AERI site, the southern Great Plains, and the time of year. Since the AERI retrievals are restricted to the infrared window region, dual D_{EFF} solutions existed. But since the AERI and lidar time series indicated that the cirrus began thin and steadily thickened, we assumed D_{EFF} started out small and grew to larger sizes. This D_{EFF} tendency assumption has no impact on the retrieval of the tunneling factor t_F.

Knowing D_{EFF} and t_F, the radiation algorithm can compute the area-weighted absorption efficiency $\bar{Q}_{ABS}$ of the size distribution for each AERI infrared microwindow. These can in turn be used to compute IWP as prescribed by Eq. (9).

The results of the 10 Nov cirrus analysis are presented in the plots below. These represent the first ground-based observations of the contribution of tunneling to absorption in ice clouds. Since the tunneling factor depends on the complexity of ice-particle shape (Baran et al., 2001), the variation of t_F in this plot may reflect variations in crystal shape. Clearly t_F is not equal to one, as is true for ice spheres; furthermore, the mean value of t_F in the following plot is 0.53 ± 0.18. D_{MEAN} in the plot refers to the mean maximum dimension of the large-particle mode of the size distribution, and is comparable to the mean dimension measured by the 2DC particle probe. Note that when D_{MEAN} climbs above 200 µm, D_{EFF} decreases slightly. This reflects an increase in concentration of the small ice crystals ($D < 100$ µm) as D_{MEAN} increases (Ivanova et al., 2001). Whether this increase is real or is an artifact of the FSSP probe remains in question.

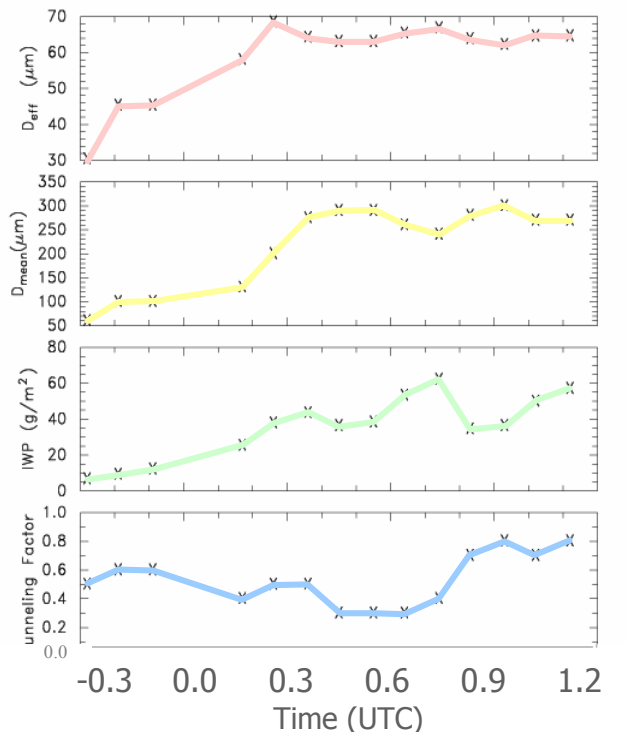

A major question is whether the high ice-particle concentrations N(D) measured by the FSSP probe are real. If the answer is "yes," then the ice particles with $D < 100$ µm account for a large portion of the SD projected area P_T, and thus will have a major impact on Q_{ABS}. This question can be resolved through

AERI observations. The difference between the exponential (top) and bimodal (bottom) curves in the plot below demonstrates the impact of the small mode on the τ_{ABS} ratio. In this Figure, it is seen that using the small mode based on the FSSP renders good agreement with the retrieved τ_{ABS} ratios (the "x" symbols) for non-convective cirrus. The vertical scatter in the measured ratios could be due to changes in ice-crystal shape, or to changes in the characteristics of the small-mode portion of the SD.

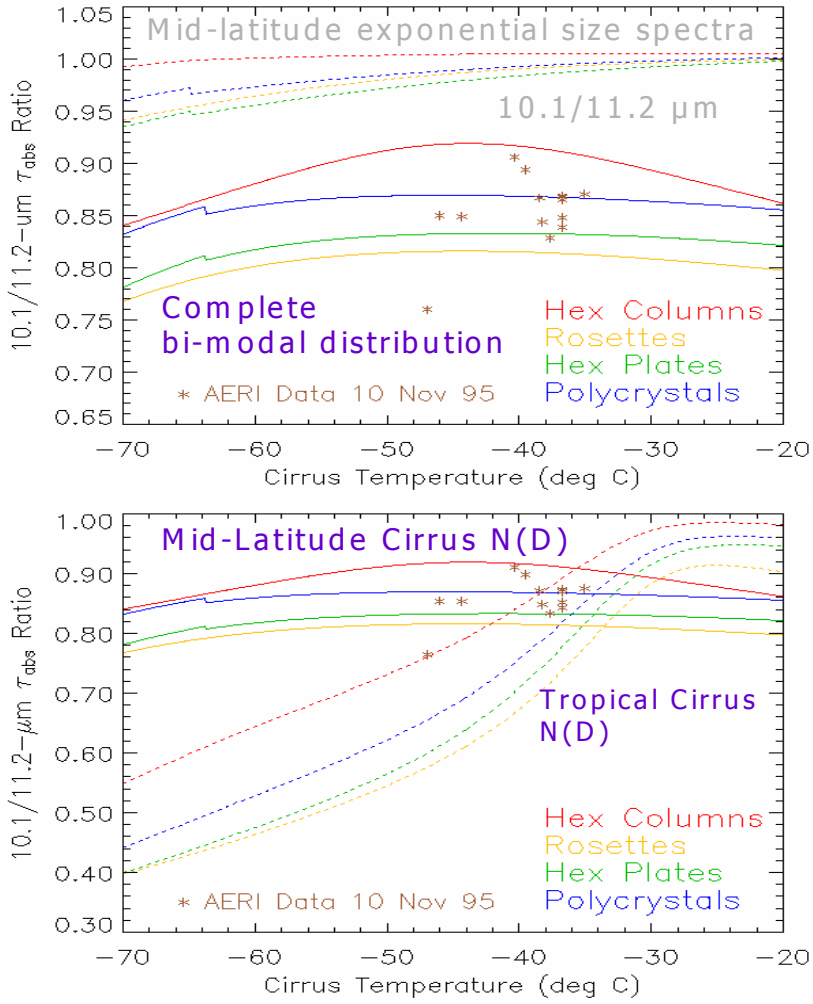

Finally, the ratio $\tau_{ABS}(10.1) / \tau_{ABS}(11.2\ \mu m)$ is predicted to behave differently as a function of temperature for tropical vs. mid-latitude cirrus (Ivanova et al., 2001; Mitchell et al., 2000). This is illustrated in the plot just above. Either MODIS satellite data or AERI data could be used to evaluate the behavior of this τ_{ABS} ratio as a function of cloud temperature for tropical and mid-latitude cirrus, thus testing the validity of these two N(D) parameterizations. The reason for the different temperature dependence is that the small-particle mode in the mid-latitude N(D) model becomes more pronounced (higher concentrations) as the large mode of the size distribution broadens. The opposite is true for tropical N(D)s, since the small mode intensifies as the large mode steepens. Hence the relative behavior of the large and small modes may be evaluated remotely.

Comparing AERI and GOES Cirrus Retrievals with 35-GHz Radar

We employed the retrieval algorithms prescribed by Eqs. (1a) and (1b) for the 9 and 13 March 2000 IOPs over the SGP site, using coincident AERI and GOES thermal infrared radiances. At first a tunneling factor of 0 was assumed; the individual AERI-based cirrus effective temperature (height) retrieval results are represented in the Figure below. It is seen that nearly half of the AERI retrievals cannot be resolved with the coincident radar observations using the zero-tunneling assumption.

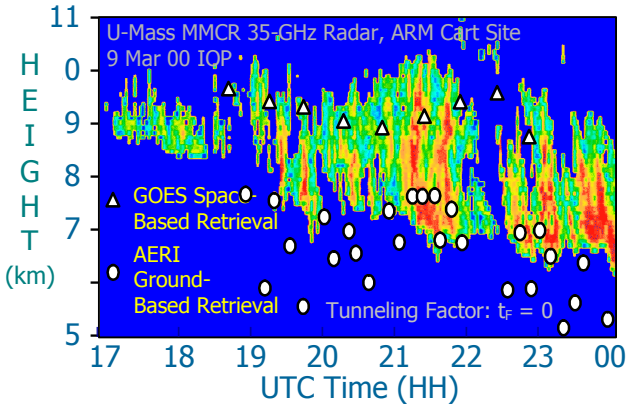

When a tunneling factor t_F of 0.6 was used to compute Q_{ABS} during the retrieval iteration process, the number of AERI retrievals that are reconcilable with MMCR observations doubled; results are shown in the Figure below. For these retrievals we used channels at 8.55 and 11 μm. This illustrates how radiances between 8 and 12 μm are sensitive to the value of t_F, and can be used to estimate the tunneling factor itself. These are among the first ground-based observations of the contribution of tunneling to absorption in ice clouds.

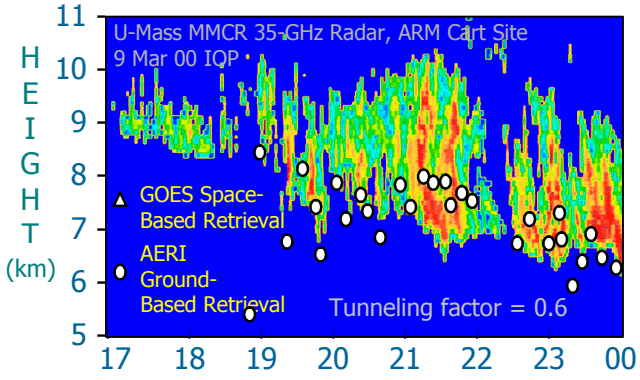

In this analysis, we chose to use the mid-latitude parameterizations because of the location of the AERI site, the southern Great Plains, and the time of year. Note too that since the lidar time series indicated that the cirrus began thin and steadily thickened, we assume that D_{EFF} started out small and grew to larger sizes. This D_{EFF} tendency assumption has no impact on the retrieval of the tunneling factor t_F.

The following four plots contain AERI (blue diamonds) and GOES (green stars) retrieval comparison plots for IWP, D_{EFF}, visible extinction optical thickness, and effective emissivity for the 9 March IOP, using a tunneling factor of 0.6.

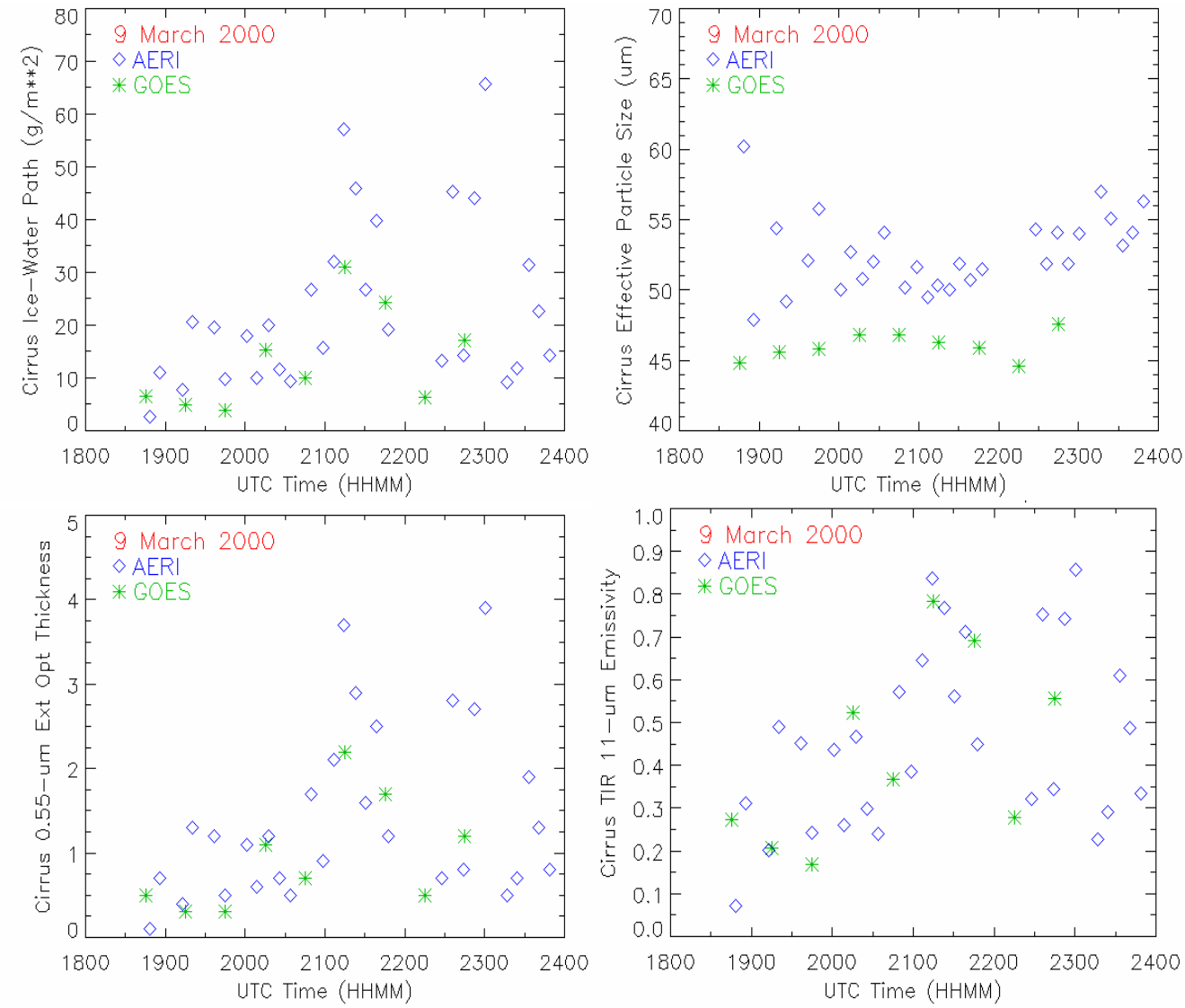

The next figure shows a time series of the GOES visible satellite image data collocated with the time series of 0.55-µm extinction optical thickness retrievals for 9 March; note how the three trends match.

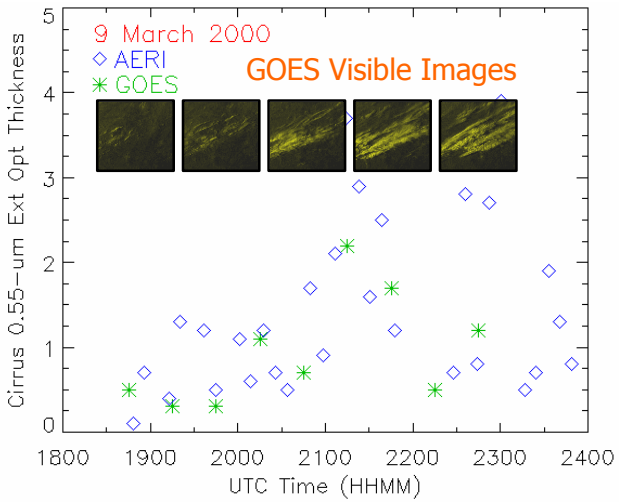

Retrievals for 13 March 2000

The Figure below shows AERI-GOES height retrieval comparisons for the 13-March IOP, collocated with the 35-GHz radar observations. The plots that follow the radar image show comparisons of microphysical retrievals in more detail, again with the MMCR radar plots inserted along the UTC time axis.

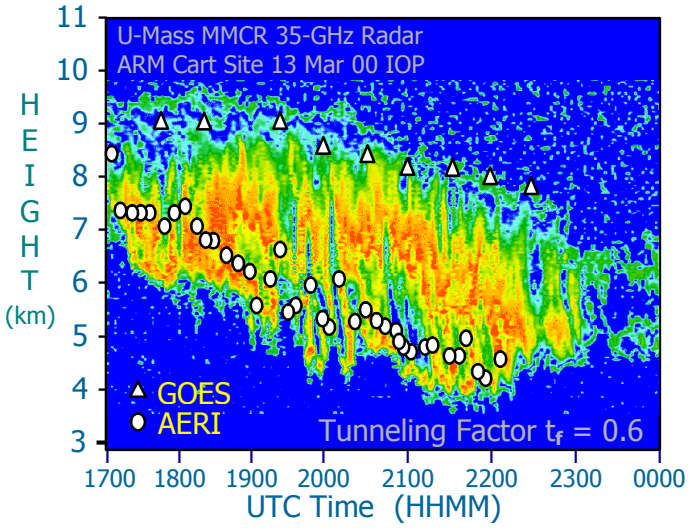

Summary

Comparisons between various methods (and data sources) such as those depicted here, each developed and funded by ARM, will continue and expand over the coming year. Preliminary comparisons indicate our ice-water path (IWP) satellite retrievals are similar to MMCR ground based retrievals for the 9 March 2000 cirrus IOP, but are less than those obtained from in situ aircraft measurements. A central focus of this study is IWP, a major predictor of the radiative forcing of cirrus clouds in climate. The

project objective is to provide a means of retrieving and comparing IWP from ground and space with relative accuracy, over the range 0-150 g/m^2.

Space-based cloud retrievals offer the most effective means for observing cirrus on truly global climate scales. However comparisons with ground-based retrievals are vital in reducing satellite uncertainties, and assessing the reliability with which satellite retrievals can be applied to the task of improving Cloud Resolving Models and subsequently understanding the influence of cirrus clouds and cloud radiative forcing on the Earth's climate system. Improving the treatment of clouds and radiation in general circulation models is one of the major goals of the ARM program.

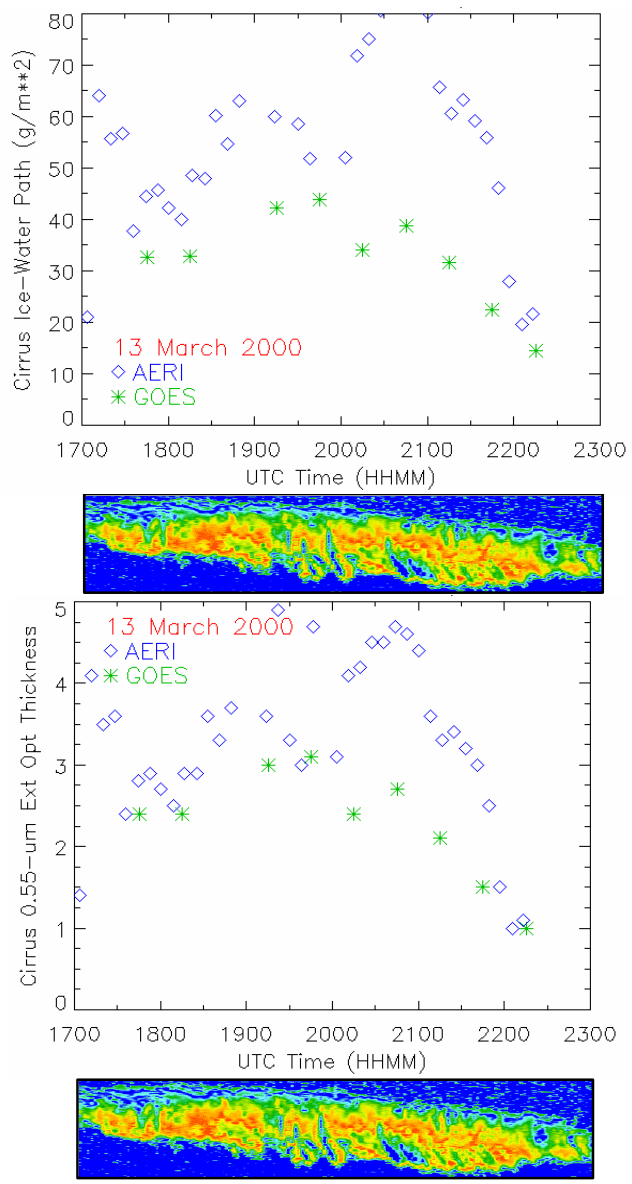

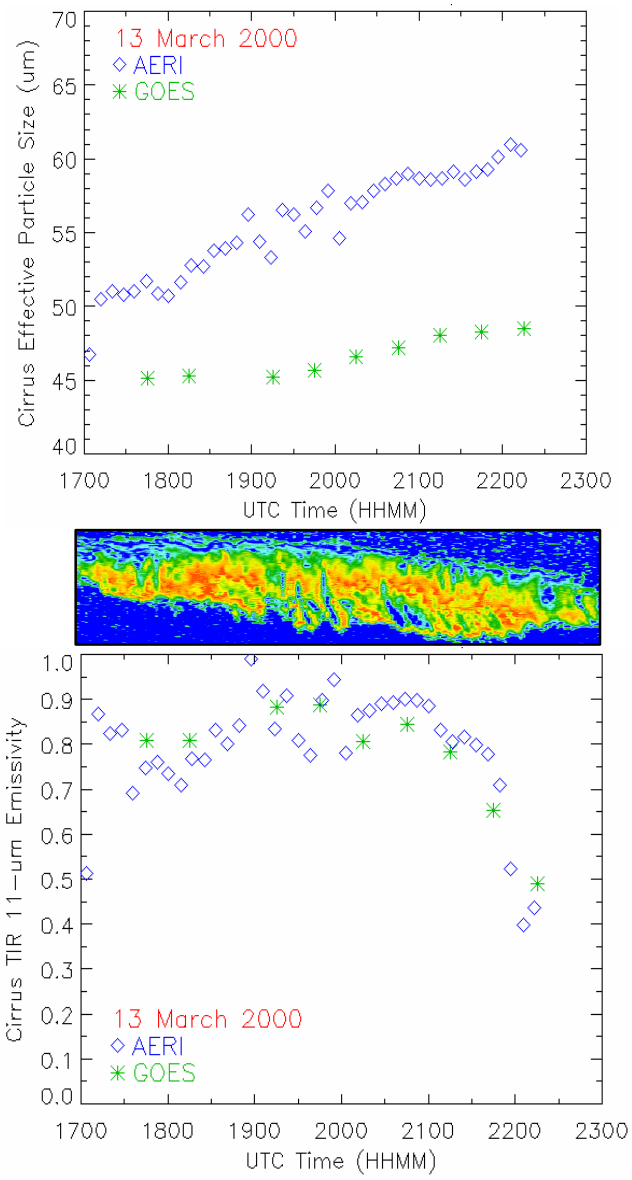

Corresponding Authors

David L. Mitchell, mitch@dri.edu,
Robert P. d'Entremont, rpd@aer.com,

References

DeSlover, D., W. L. Smith, P. K. Ppiironen, and E. W. Eloranta, 1999: A methodology for measuring cirrus cloud visible-to-infrared optical depth ratios. *Journ. Atmos. Ocean*, Tech., **16**, 251-262.

Heymsfield, A. J., and C. M. R. Platt, 1984: A parameterization of the particle size spectrum of ice clouds in terms of the ambient temperature and the ice water content. *Journ. Atmos. Sci.,* **41**, 846-855.

Ivanova, D., D. L. Mitchell, W. P. Arnott, and M. Poellot, 2000: A GCM parameterization of bimodal size spectra and ice-mass removal rates in mid-latitude cirrus clouds. *Atmos. Res*., **59**, 89-113.

McFarquhar, G. M., and A. J. Heymsfield, 1997: Parameterization of tropical ice-crystal size distributions and implications for radiative transfer: results from CEPEX. *Journ. Atmos. Sci.*, **54**, 2187-2200.

Mitchell, D. L., D. Ivanova, A. Macke, and G. M. McFarquhar, 2000: A GCM Parameterization of bimodal size spectra for ice clouds. *Proceedings of the 9th ARM Science Team Meeting*, March 22-26, 1999, San Antonio. (www.arm.gov/docs/documents)

Mitchell, D. L., W. P. Arnott, C. Schmitt, A. J. Baran, S. Haveman, and Q. Fu, 2001: Contributions of photon tunneling to extinction in laboratory-grown hexagonal columns. *Journ. Quant. Spectroscopy and Rad. Transf*., **70**, 761-776.

Mitchell, D. L., and A. J. Baran, 2002: Testing of the Modified Anomalous diffraction approximation with T-matrix calculations for hexagonal ice columns. *Conference Atmospheric Radiation*, Amer. Meteor. Soc., Jun 3-7, 2002, Ogden UT, J139-144.

Mitchell, D. L., R. P. d'Entremont, D. H. DeSlover and W. P. Arnott, 2003: Multispectral thermal retrievals of size distribution shape, effective size, ice water path, optical depth and photon tunneling contribution. *12th Conference on Satellite Meteorology and Oceanography*, AMS Annual Meeting, Long Beach, California, Feb. 9-13, 2003.

Mitchell, D. L., A. Macke, and Y. Liu, 1996: Modeling cirrus clouds. Part II: Treatment of radiative properties. *J Atmos Sci,* **53**, 2967-2988.

Twohy, C. H., A. J. Schanot, and W. A. Cooper, 1997: Measurement of condensed water content in liquid and ice clouds using an airborne counterflow virtual impactor. *J Atmos Ocean Tech*, **14**, 197-202.